CONCEPT, DEVELOPMENT AND BREADBOARD TESTING OF INNOVATIVE LAUNCH ADAPTER RING MODULAR GRIPPER (LAR-MG) FOR SATELLITE ROBOTIC CAPTURE.

Jacek Musiał [(1)], Tomasz Kowalski[(2)], Konrad Aleksiejuk[(2)], Adam Sikorski[(2)]

[(1)] *Institute of Aviation, Lukasiewicz Research Network, al. Krakowska 110/114, 02-256 Warsaw, Poland, Email:jacek.musial@ilot.lukasiewicz.gov.pl*
[(2)] *Space Research Centre, Polish Academy of Sciences, ul. Bartycka 18a, 00-716 Warsaw, Poland, Email:tkowalski@cbk.waw.pl*

ABSTRACT

This paper describes a LAR gripper breadboard developed for use in the SpaRoC project, where it was used for testing robotic capture operations in microgravity conditions, and therefore it was itself successfully tested. Innovative mechanism layout allowed for achieving, among other features, ultra - wide allowable initial position error and mechanical simplicity.

Testing consisted of verification of capture misalignment envelope and functional tests on air bearing table, as part of noncooperative satellite capturing system.

1 INTRODUCTION

On-orbit servicing and active debris removal missions are topics of an increasing interest [1]. One of main planned approaches rely on the use of unmanned satellite equipped with a manipulator with gripper, usually intend to catch and hold launch adapter ring (LAR) of target satellite. This approach was baseline in project SpaRoC (Development and validation of control system for space manipulator), funded by Polish National Center for Research and Development. Validation in this case meant tests in planar microgravity conditions – on air bearing table, in microgravity laboratory at Space Research Centre (CBK).

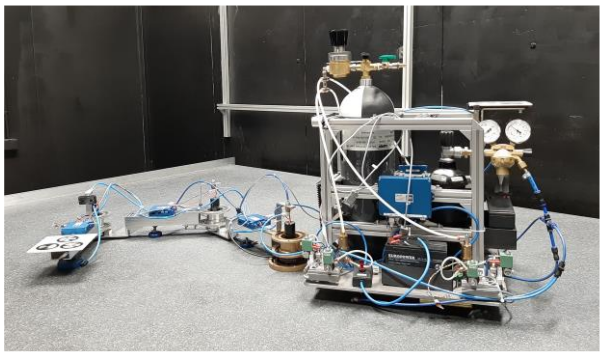

Figure 1. Test stand before upgrade – satellite mock-up platform with 3DoF robotic arm, floating via air bearings on granite table.

To perform these tests, it was necessary to upgrade existing test setup (Satellite mock-up platform with 3DoF robotic arm – Fig.1) by introducing LAR gripper and target satellite mock-up platform with LAR (Fig. 2).

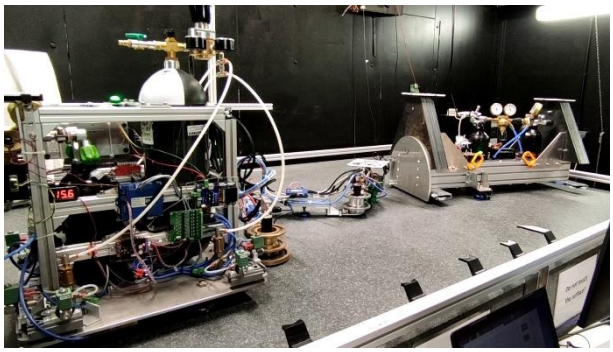

Figure 2. Test stand after upgrade – target satellite mock-up platform visible on the right.

At the time of project realisation, there was no known mature design of a LAR gripper, that would justify designing system for using such design. Instead it was decided, that such gripper breadboard must be developed, that would fulfil i.e. following requirements:

- Grip scaled down (0.3:1) LAR section
- Allow for as high as possible linear and angular misalignment
- Remain holding when unpowered
- Allow for multiple capture attempts

Gripper breadboard had to be scaled same way as the rest of the experiment, in order to be representative. Driving parameters were on one hand: platform mass, robotic arm link length and joint stiffness, and on the other hand – corresponding values of robotic arm developed in CBK in LEMUR project, and assumed mass of chaser satellite (Tab. 1).

Parameter	Initial	Scaled	Scale Ratio
Chaser mass [kg]	720	72	0,100
Link length [mm]	1500	449	0,299
Joint stiffness [Nm/mrad]	25,8	4,7	0,182

Table 1. Scaling requirements

For experiment to be consistent, scaling ratios must fulfil the same relations, as their physical quantities. In this case, they are as in Tab. 2.

Quantity	Symbol	Expression	Value
Time	k_T	(base)	0.222
Length	k_L	(base)	0.299
Mass	k_M	(base)	0.100
Velocity	k_v	k_L/k_T	1.35
Acceleration	k_a	k_L/k_T^2	6.08
Angular velocity	k_ω	$1/k_T$	4.51
Angular acceleration	k_ε	$1/k_T^2$	20.3
Force	k_F	$k_M k_a$	0.609
Stress (pressure)	k_σ	k_F/k_L^2	6.81
Density	k_ρ	k_M/k_L^3	3.74
Torque	k_t	$k_F k_L$	0.182
Inertia	k_J	$k_M k_L^2$	0.00897

Table 1. Scaling ratios. Driving ones are in bold.

As it turns out, demands for scaled gripper were higher than for full-sized one. In particular, almost sevenfold increase of stress and modulus of elasticity was required. Fulfilling these exactly was not possible, so gripper was designed in reduced version only, but using steel where aluminium alloys would be expected.

As target interface, CASA CRSS 1194 SRF adapter ring was chosen (Pic. 3), as it is widespread solution of known geometry.

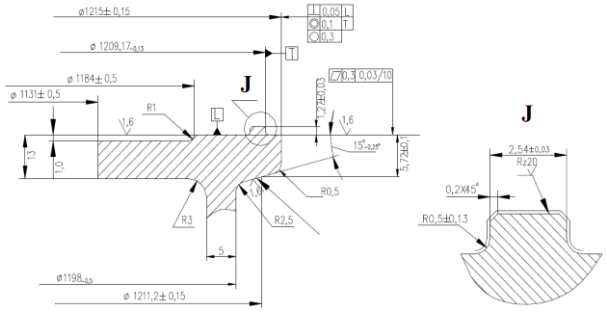

Figure 3. CASA CRSS 1194 SRF adapter ring geometry (adapter side), full scale.

2 DESIGN

Most of revealed existing designs [2, 3, 4] were based on linear motion, vice-like mechanisms. Linear motion requires relatively (to rotary motion with same load) heavy hardware and is more prone to failure, and vice-like clamping require small initial misalignment. Also, to achieve holding when unpowered, either locking mechanism is required (that increase complexity), or non-back driveable (e.g. trapezoid lead screw), and thus low efficiency drive.

To combat these issues, alternative approach was chosen. Base of design is concept of tentacle units [Fig. 4]. Driven by crank and erected by spring force, tentacle arm grabs target corner and pulls it towards hardstop, where target is fixated with strong force, utilizing crank dead centre. Simplified scheme of 2D application with 2 tentacle units is shown on Fig. 5.

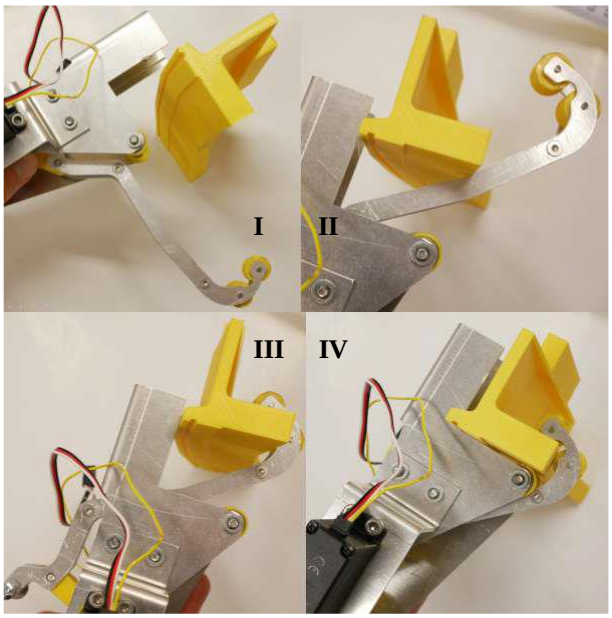

Figure 4. Early proof of concept single tentacle unit, and its phases of capturing – open, soft contact, pulling, holding.

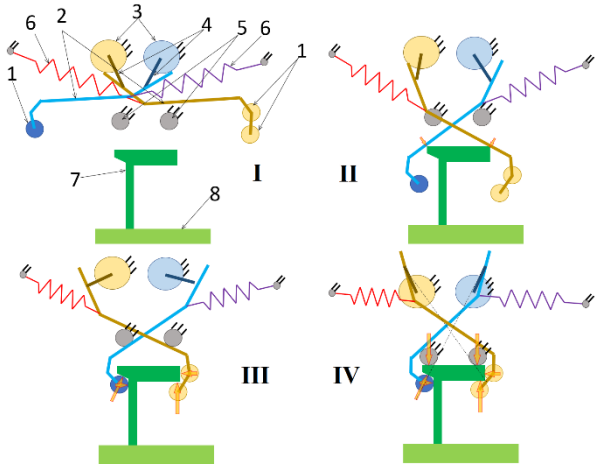

Figure 5. Principle of operation in 2D. 1 - contacting element, 2 - arm, 3 - motor, 4 - crank, 5 - hardstop, 6 - erecting spring, 7 - LAR section, 8 - Spacecraft.

It was decided to capture the LAR with three tentacle units, in three points along a short section on one side of the ring – two side points from the inside of the ring and one central point from the outside – due to the compactness of such an approach and the anticipated better tolerance for angular misalignment. This solution

makes it more difficult to transfer bending moments due to the short gripping arm compared to capturing the LAR at points farther apart. It was assumed that the LAR should withstand a bending moment load of 18 Nm, as this is the maximum that could be generated by the robotic arm drives.

The mechanical design was carried out with the assumption of maximum simplicity and ease of manufacturing to accelerate the iteration of subsequent versions. Most components were either laser-cut or 3D printed using FDM technology. Commercial off the shelf high-ratio reduction gear DC motors and electromechanical limit switches were used as actuators. To detect whether the LAR is in gripping range, an inductive proximity sensor signal was used for simplicity, as can be seen in Fig. 13.

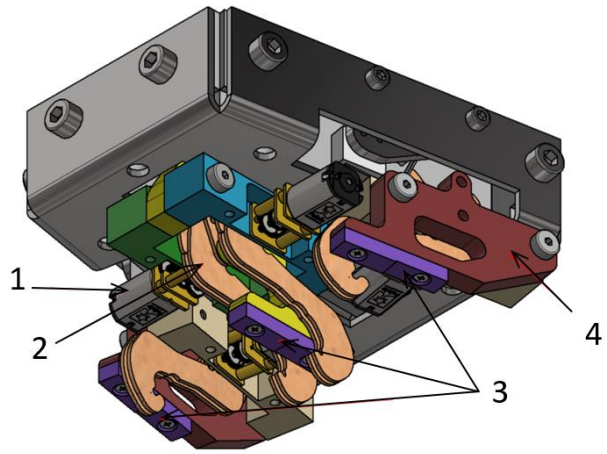

Figure 6 - Mechanical design of the LAR-MG. 1- DC Gearmotor, 2 – central tentacle arm, 3 – hardstops, 4 – side tentacle unit.

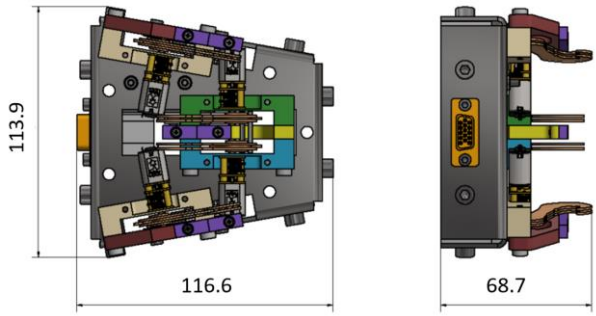

Figure 7 – Dimensions

The designed gripper weighed approximately 1.05 kg, with the tentacle units weighing less than 0.5 kg, and almost 0.6 kg accounting for the structure to which they are attached.

The gripping range of such a system does not have a regular shape and varies depending on the rotation angle of the LAR. For each individual tentacle, the gripping range is a circle with its centre located on the crank axis of rotation and a radius equal to the reach of the gripper. In the planar case, the gripping area is the intersection of these circles, limited to the half-space determined by the hard stops (Fig. 8).

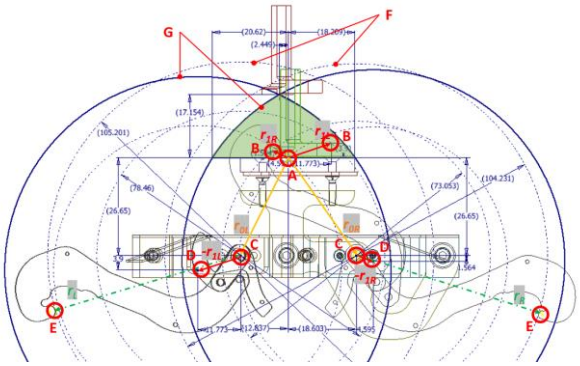

Figure 8 - Gripping range for a LAR rotation angle of 0 degrees. The gripping area is similar to an unequal-sided triangle, with a base of 38.8mm and a height of 17.2mm (130x57mm at full scale).

The manufactured gripper and a section of the LAR for testing purposes are shown in Fig. 9, 10. The photos depict the design after modifications were made to increase its reliability and gripping area.

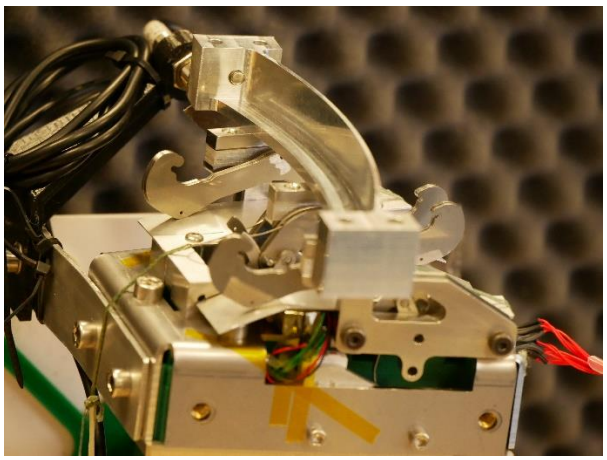

Figure 9. LAR-MG (open) with LAR fragment

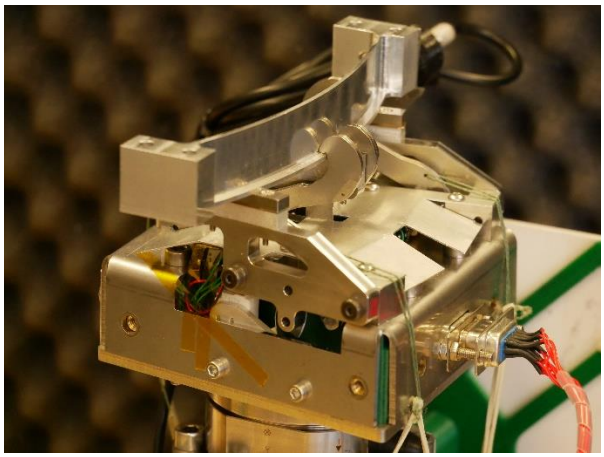

Figure 10. LAR-MG (closed) with LAR fragment.

3 TESTS

Two groups of tests were conducted: experimental determination of the gripping range, necessary for the manufacturing of counterpart of the inductive sensor, and a comprehensive system test campaign under simulated microgravity conditions.

3.1 Gripping Range Tests

Gripping range tests were carried out on a simple setup that allowed LAR for planar motion with friction while immobilizing the gripper (Fig. 11). In a series of measurements, the boundaries of proper gripping zone were determined for various distances between the LAR and the hard stops plane. The initial position was defined in a coordinate system aligned with the LAR in the fully grasped position: the Y-axis in the axial direction and the X-axis in the radial direction, on the table plane, with the point (0,0) corresponding to zero displacement.

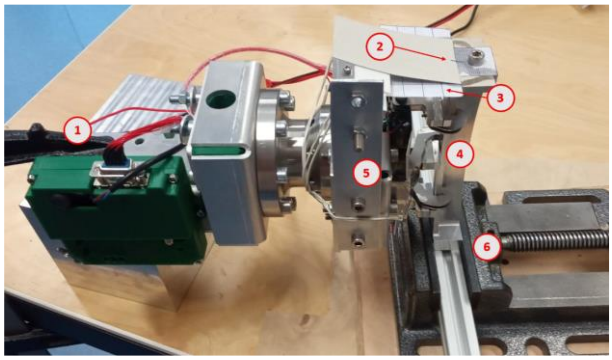

Figure 11. Test stand. 1 – LAR-MG fixture, 2 – marker, 3 – milimiter paper, 4 – LAR, 5 – LAR-MG, 6 – vice, freely moving on the table.

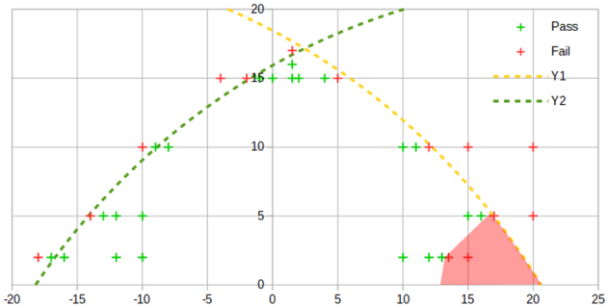

Figure 12. Results for a rotation angle of 0 degrees. Green marks indicate proper gripping, while red marks indicate improper gripping. Dashed lines mark the predicted gripping range of the outer and inner grippers. An anomaly is visible in the vicinity of (x,y) = (15, 2).

The tests demonstrated good repeatability and agreement with the predictions. Various imperfections in the design were identified and addressed during the test campaign. The discrepancy observed in the area of (x,y) = (15, 2) between the tests and the predictions resulted from a different nature of improper gripping - the LAR was properly grasped by the tentacles but was being pulled sideways towards the hard stop. This can be easily resolved by widening the hard stops, but it was considered unnecessary at this stage, as the gripping range was sufficient for the final test campaign.

Tests were also conducted for an inclination of ±20% (11.3 degrees), but not for all distances. In the presented simple setup, precise angular positioning was challenging, resulting in less repeatable results. However, rotating the LAR by such an angle caused not a reduction in the gripping area, but rather its displacement along the x-direction..

It is worth noting that the gripping range (measured: 33 x 16 mm) is several times larger than the size of the LAR foot (12.6 x 3.9 mm) that is being gripped - corresponding to an area of 110 x 53 mm at full scale.

3.2 System tests in microgravity

The primary goal of the microgravity tests was to test the control algorithms developed within the SpaRoC project, with the LAR-MG gripper serving as a tool for that purpose. However, the gripper itself was also tested during the test campaign, although it was not specifically dedicated to it.

The microgravity laboratory is equipped with a 2x3m granite table designed to work with air bearings, allowing objects to move on it with minimal friction. The entire table area is monitored by a vision system that tracks the positions of markers within that area.

The experimental setup consisted of:
1. A 72 kg chaser satellite mock-up on air bearings, with a 3DoF planar manipulator and the LAR-MG gripper attached to the last link. The gripper was mounted through 6-axis force and torque sensor.
2. A 153.5 kg mock-up of the target satellite with a mounted LAR ring segment.

The force sensor used was piezoelectric, measuring forces and torques at a frequency of 1 kHz with 4 channels – forces and torque in the table plane, and also force perpendicular to the plane to verify forces beyond the planar case (Fig. 13, 14)

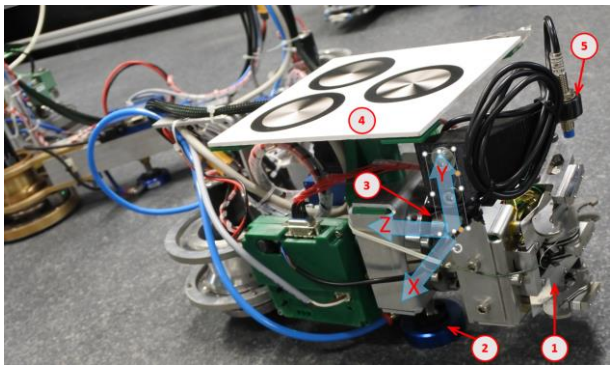

Figure 13. Gripper in system test configuration, mounted on robotic arm. 1 - LAR-MG, 2 – air bearing, 3 – froce/torque sensor with its coordinate system, 4 – vision system marker, 5 – induction sensor.

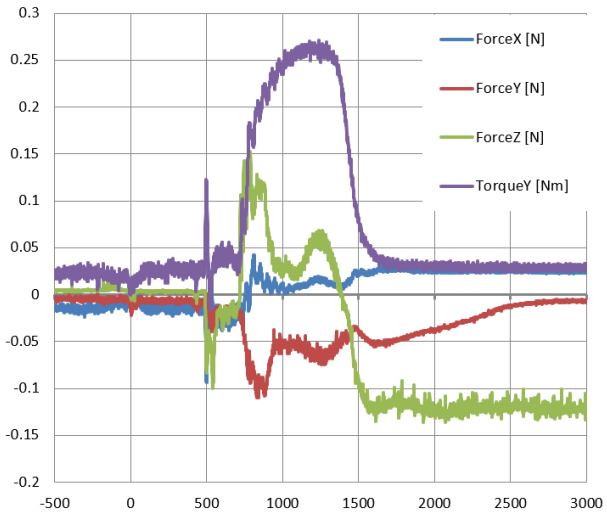

Figure 13. An example of measured force and torques. 0ms – triggering of capturing sequence, 500ms – soft contact, 750ms – start of pulling, 1700ms – holding. The negative force in the Z direction after gripping is due to centrifugal force exerted on the rotating system of the two satellites.

The standard gripping algorithm follows these steps: approach the nominal position, verify the position using the proximity sensor, and trigger the gripper. However, due to the high aspect ratio of the effective gripping area, this approach was not considered the best strategy. It would only allow for an error of approximately 8mm in worst direction, which corresponds to the radius of the inscribed circle within the gripping area.

An alternative method was chosen, where the gripper approached the target point along the LAR axis, and the gripper was triggered as soon as the induction sensor detected proximity to the triggering plate, which had a shape similar to the effective gripping area. This approach doubled the permissible error, allowing for a deviation of up to 16.5mm from the desired path, which is half the width of the gripping range.

During the test campaign, the gripper successfully performed its task, effectively gripping the target in all 27 cases when properly triggered. This not only confirmed the effectiveness of the gripper mechanism but also validated the chosen gripping strategy.

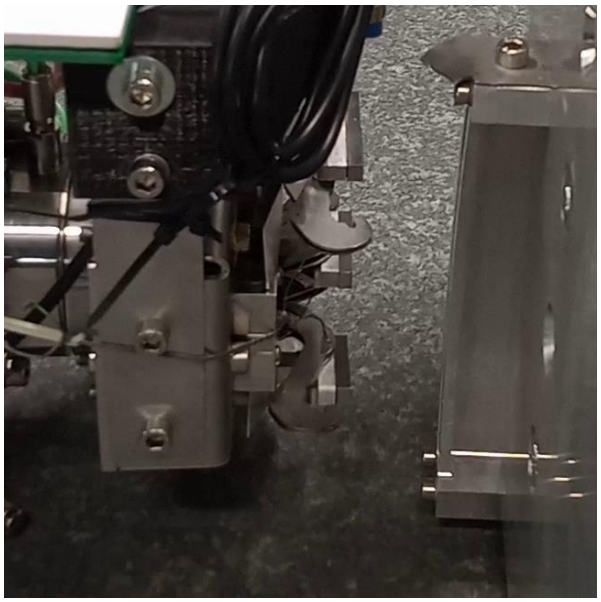

Figure 14. Phase I – open, at distance. Proximity sensor counterpart visible, bolted atop LAR segment.

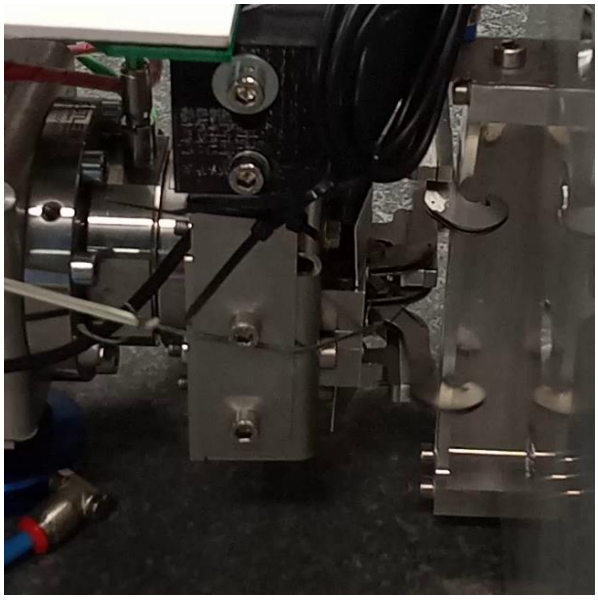

Figure 15. Phase II, soft contact. During this phase LAR enters no-escape zone.

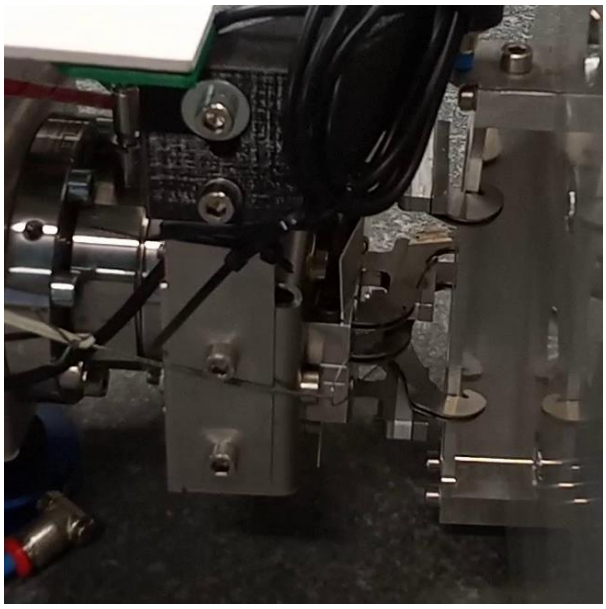

Figure 16. Phase III – pulling.

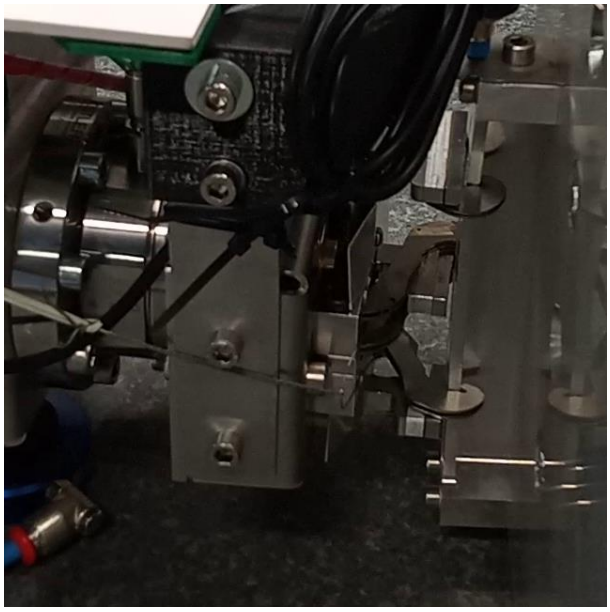

Figure 17. Phase IV - holding

4 SUMMARY

According to the ESA definition, the tests conducted on the reduced scale breadboard under relevant conditions qualify it as TRL5. As it was not the primary objective of the project, the gripper was not tested at all important aspects (i.e. verification of holding forces and stiffnesses) although it underwent a successful testing campaign within a larger system, effectively fulfilling its tasks.

Advancing to TRL6 should not pose a problem. From the gripper's perspective, the scaled experiment added complexity to the project, as the scaling for microgravity tests significantly increased the gripper's loads and required power densities, while its small dimensions made integration challenging, especially regarding components such as limit switches and springs.

The tests on the granite table were performed in a reduced, flat case. However, the LAR-MG breadboard is three-dimensional and functions just as well when not constrained remaining three degrees of relative movement by the table. The tests on the table were conducted in the most unfavourable gripper orientation, ensuring high sensitivity to position errors while minimizing transmittable moments. If the LAR segment were placed horizontally, all these aspects would be considerably simpler.

Commonly available materials and products were used in the project, nevertheless resulting in a functioning device. If required, designing and constructing a version with high-tech components should not be an issue, especially considering that the project was scaled down, and further direct development would not yield any benefits.

In case there is a need for further project development, the key issues to address are as follows:

1. Increasing the tolerance to LAR inaccuracies: Not all gripped surfaces are tightly tolerated, and the current solution is sensitive to such deviations, which can lead to incomplete closure or loose grip even after closure. It may be necessary to introduce additional flexibility or a short-stroke tensioning drive.

2. Developing a position sensing system that works in real-world scenarios where there is no specially prepared contact plate for the proximity sensor. There are preliminary concepts for individual optical sensors for each finger, determining whether it is in a gripping position, but there is still a long way to go from an idea to a functional system.

A significant advantage, besides the wide capture range, is the modularity of the system. It allows for easy adaptation to different LAR diameters, different angular placement of gripping points based on requirements, and the introduction of redundancy by adding extra fingers. When in the open position, these fingers do not occupy the half-space where the LAR could be located. Furthermore, the system can be used not only for end effector gripping but also for solid docking to the LAR ring by placing multiple finger modules around the LAR circumference.

This paper was partially supported by the Polish National Center for Research and Development project no. LIDER/19/0117/L-10/18/NCBR/2019.

5 REFERENCES

1. W.-J. Li, D.-Y. Cheng, X.-G. Liu, Y.-B. Wang, W.-H. Shi, Z.-X. Tang, F. Gao, F.-M. Zeng, H.-Y. Chai, W.-B. Luo, Q. Cong and Z.-L. Gao, "On-orbit service (OOS) of spacecraft: A review of engineering developments," Prog. Aerosp. Sci. 108, 32–120 (2019).

2. Gerrit Hausmann et al., E.DEORBIT Mission: Ohb Debris Removal Concepts, Conference: ASTRA 2015 - 13th Symposium on Advanced Space Technologies in Robotics and Automation

3. Steffen Jaekel et al., Design and Operational Elements of the Robotic Subsystem for the e.deorbit Debris Removal Mission, Frontiers in Robotics and AI, 2018.

4. Grzegorz Stachyra, Gripper for in-orbit servicing operations, Proc. 8th European Conference on Space Debris (virtual), Darmstadt, Germany, 20–23 April 2021, published by the ESA Space Debris Office